

A RANGEFINDER WITH FAST MULTIPLE RANGE CAPABILITY

J. M. Payne, D. Parker and R. Bradley

National Radio Astronomy Observatory*

2015 Ivy Road

Charlottesville, Virginia 22903

ABSTRACT

A rangefinder is described that uses the propagation time of a beam of infrared radiation to measure distances of up to 120 m with errors of less than 50 microns. The instrument is capable of measuring up to five different distances per second by directing an amplitude modulated infrared beam to a retroreflector located at the far end of each path. The instrument is being tested with the expectation that such a system could be used to make precise and rapid measurements on a large radio telescope. Such measurements would be used to adjust the shape of the telescope reflector surface to correct for thermal and gravitational deformations taking place during astronomical observations. It is possible that the measuring system could be extended to relate the positions of certain moving parts of the structure to a reference system fixed in the ground, thus opening the possibility of making corrections to the telescope pointing.

*The National Radio Astronomy Observatory is operated by Associated Universities, Inc. under cooperative agreement with the National Science Foundation.

INTRODUCTION

The National Radio Astronomy Observatory (NRAO) is constructing a fully-steerable radio telescope at Green Bank, West Virginia, to be known as the Green Bank Telescope (GBT). The telescope design provides a reflector surface which is a part of a paraboloid, so positioned that radiation can reach the reflector and then pass to one of two focal points without meeting any obstructions. This clear aperture collects radiation from a circular area of 100 meters diameter. The goal of the design is to have an instrument which performs well at radio wavelengths down to 6 mm. It may be possible in the future to lower this short-wavelength limit to 3 mm; this depends on several factors, one of which is the outcome of the present work.

To achieve satisfactory performance at short wavelengths, a radio telescope must meet two main requirements:

- The reflector surface must maintain its required shape.
- The position of the telescope beam on the sky must always be controlled with precision.

These can be thought of as the "surface" and "pointing" requirements; the precision with which they must be met is related to the shortest wavelength at which the telescope is to be used, and both are very dependent on the environmental conditions at the telescope site. As an example, if the GBT were being used at a wavelength of 3 mm, it would be expected to have a surface whose departures in shape from perfection had an RMS value of at most 0.2 mm, and the astronomer would wish to point the telescope beam to within one arcsecond of any desired point in the sky.

The most significant environmental effects are due to wind and temperature. Even in the absence of wind, unavoidable temperature variations

result in a short wavelength limit of approximately 8 mm for a steel structure the size of the GBT. Winds can somewhat reduce temperature differentials across the structure, but wind is a major enemy of good pointing. As the telescope moves in elevation, many parts of the structure deform as the relative direction of the force of gravity changes. Although these deformations can to some extent be computed, it is not easy to allow for all their effects.

A rangefinder system for the GBT, based on the design outlined in this paper, is being planned to carry out the following tasks:

- To measure the shape of the reflector surface and to correct for changes due to gravity and thermal effects.
- To relate the positions of all the measured surface points to a reference frame of points fixed in the ground around the telescope.

The reflector surface of the GBT has been designed to facilitate the measurement and adjustment of the surface. 2,004 accurately made reflective panels are mounted onto a steel backup structure, the surface of each panel deviating from the required parabolic surface by less than 75 microns RMS. In order to maintain the correct surface shape in the presence of deformations in the backup structure, connections between the surface panels and backup structure are made through linear actuators located at each junction of four panel corners. The reflecting surface is then a continuous sheet that may be adjusted to remove both the gravitationally-induced deformations resulting from tilting the telescope and thermally-induced changes in the backup structure. These deformations will change slowly compared to the speed at which the surface can be measured. Wind-induced deformations, however, will be too rapid to be corrected by movements in the main surface so, at least in

the early years of operation, short wavelength operation will be restricted to calm conditions.

The proposed metrology system for measuring the surface of the antenna is shown in Figure 1. Three rangefinders located on the feed arm support will measure the distance to every one of 2,209 retroreflectors, each one of which is located directly above a surface adjusting actuator. Each rangefinder may measure a distance to a surface retroreflector and also to each of its neighboring rangefinders. The range data will then be processed in a computer to give the best-fit paraboloid surface. The adjustment required at each actuator to correct the departure from the best-fit surface will then be calculated and sent as a command to the actuator.

At its shortest operating wavelength, the GBT will have a diffraction beam of approximately seven arcseconds and accurate pointing of this beam presents a formidable problem. The determination of the best-fit surface is the first step towards a solution, since this means that the location of the paraboloid and the direction of its axis are known in reference to the surface measuring rangefinders. The position of these rangefinders with respect to fixed points on the ground will be derived using measurements from 12 ground-based rangefinders surrounding the telescope. If these ranges are known to an accuracy of 50 microns, the telescope beam direction will be known to an accuracy of approximately one arcsecond over most of the sky.

The specifications for the rangefinder result from the requirements of both accuracy and measurement speed. The accuracy requirement is straightforward and stems from the precision required in the surface setting and pointing. The speed of measurement is dictated by the rate at which the ranges to be measured are changing due to thermal effects and the excitation

of various modes of oscillation of the telescope structure. An instrument with an accuracy of 50 microns for ranges up to 120 m, capable of measuring five ranges per second, is needed to meet these requirements.

Many commercial rangefinders are available [1], but none of these come close to meeting the required accuracy. Several experimental instruments have been constructed [2], [3], but none have demonstrated both the required speed and accuracy in an outdoor environment. The instrument described in this paper demonstrates both improved accuracy and speed over previous instruments. The improved accuracy is a result of increased modulation frequency, made possible by the availability of low-cost laser diodes developed for the consumer electronics industry. The improved measurement speed stems from a high signal-to-noise ratio, the result of higher modulated power levels and a more sensitive detector. This is aided by the digital signal processing now available using inexpensive personal computer technology.

DESCRIPTION OF INSTRUMENT

Principle of Operation:

The principle of operation of the method is shown in Figure 2. An intensity modulated light beam is transmitted over the path to be measured, is reversed in direction by a retroreflector at the far end of the path, and is returned to the instrument. The phase of the intensity modulation envelope of the returned beam is retarded with respect to the phase of the outgoing beam by $2d/\lambda$ where d is the distance to be measured and λ is the wavelength of the intensity modulation envelope and depends on the group refractive index of the atmosphere. If $\lambda < 2d$, the phase will be retarded by more than one cycle and ambiguities in distance reading arise. The phase detector output in Figure 2 is proportional to $\phi_s - \phi_R$ where ϕ_R is a constant and $\phi_s = 2d/\lambda$ radians. The

phase detector output repeats every 2π radians and will be $\phi_s = \frac{2d - n\lambda}{\lambda} \times 2\pi$ where $(2d - n\lambda) < \lambda$ and n is an integer.

The instrument described here uses a modulating frequency of 1.5 GHz so the output of the phase detector will repeat every 10 cm. In some applications, this ambiguity is resolved by a change of modulation wavelength but here all distances should be known well enough so that resolving the ambiguity is unimportant.

Block Diagram of Instrument:

A detailed block diagram of the instrument is shown in Figure 3. The transmitter is a laser diode emitting at a wavelength of 780 nm. Sinusoidal variation of the current through the diode modulates the intensity of the transmitted beam which is directed to the distant retroreflector by a series of mirrors. The final mirror is a computer-controlled beam steering mirror which also accepts the expanded returned beam from the retroreflector. Careful optical alignment ensures that the transmitted and received beams are coaxial. The divergence of the transmitted beam is such that the beam received at the distant retroreflector has a diameter several times that of the retroreflector. Consequently, positioning of the light beam with respect to the retroreflector is not critical; an angular positional accuracy of 20 arcseconds is more than adequate.

The returning light beam is focused onto a fast silicon detector, the resulting electrical signal is amplified and then mixed with a frequency offset from the transmitter frequency by 1 kHz. The phase of the resultant 1 kHz intermediate frequency is directly related to the phase of the 1.5 GHz modulation envelope of the returned signal and is a measure of the path length

to the retroreflector with the restriction of the ambiguity previously mentioned.

In order to calibrate slow drifts of the zero point of the instrument, the beam steering mirror is used to measure a reference path within the instrument at regular intervals. One calibration measurement per minute is sufficient to reduce the zero point error to less than five microns.

The beam steering mirror is controlled by a personal computer that also calculates the phase difference between the 1 kHz reference frequency and the 1 kHz intermediate frequency. This instrument computer can act in a stand-alone mode or may be controlled via a serial link from a central computer. A typical sequence of operations would be for the central computer to issue a series of retroreflector positions, the instrument computer then drives the beam steering mirror to the first of these, computes a range, stores the result and moves on to the next retroreflector. At the end of the sequence, all the measurements are passed to the central computer.

The instrument uses several commercially-available parts, but some components especially critical to its performance deserve a more detailed description than given above.

The Transmitter:

The output of the transmitter laser diode is modulated by varying the bias current about a fixed dc value. The matching and bias circuitry is shown in Figure 4. To obtain a usable modulation depth, the 1.5 GHz RF modulating signal must be power matched to the diode impedance (~ 10 ohms) in the presence of the parasitic capacitance and inductance associated with the diode package. The package lead inductance is series resonated at 1.5 GHz using a chip capacitor. The dc bias is supplied to the diode through a RF

choke. The diode impedance is transformed to 50 ohms using a microstrip quarter-wave transformer. A return loss of less than -15 dB was measured at the transmitter RF input port. A modulation depth for a RF drive level at 1 mW is estimated to be 30%. The laser diode and all associated biasing components are contained in a well-shielded enclosure. The collimated 1.5 x 2.0 mm beam emerges from the transmitter through a small aperture.

The Receiver:

The circuit diagram for the receiver is shown in Figure 5. The receiver consists of a photodetector, RF amplifier (20 dB) and double-balanced mixer. The 1 kHz IF signal, which is dc isolated from the mixer, is further amplified (x300) using low-noise op-amp circuits. The RF components are interconnected using 50 Ω microstrip and all the components are mounted within a metallic enclosure. Particular care was taken to filter all power supply connections.

Leakage of signals at the transmitter frequency into the receiver circuits is highly undesirable and will lead to a nonlinear response to changes in target distance. In order to keep the resulting errors below 10 microns, any leakage signal at the phase detector must be less than one-thousandth of the voltage resulting from the optical return signal. This level of isolation requires some care in design and construction.

The Oscillator Circuits:

The phase of the returned signal is measured using digital signal processing techniques. To achieve an accurate measure of the phase, the 1 kHz IF signal is sampled at 64 samples per cycle, thus requiring high spectral purity for both the 1.5 GHz transmitter and the 1.5 GHz + 1 kHz local oscillator. Any noise on either of these two oscillators at a frequency

offset 1 kHz from the desired frequency will add noise to the 1 kHz intermediate frequency and, consequently, degrade the accuracy of the range measurement.

Another requirement in the design of the oscillator system is that of absolute stability. An accuracy of 10 microns in a range of 120 m is better than 1 part in 10^7 , so the stability of the oscillators must be greater than this. A hydrogen maser was available at the site where the instrument was tested so the 100 MHz output from the maser was used as the frequency standard, giving a long-term stability of 1 part in 10^{15} .

The oscillator circuits are shown in Figure 6. A commercially-available X15 multiplier accepts the 100 MHz standard and outputs a stable 1.5 GHz modulating signal to the laser diode. A 1 kHz signal internally generated in the instrument's computer serves to offset the local oscillator from the transmitter frequency by 1 kHz and is also used as the reference against which the phase of the returned signal is compared. The local oscillator frequency is generated by a voltage-controlled crystal oscillator. A phase-lock loop using the reference signal as an offset frequency locks this oscillator to 1 kHz above the 1.5 GHz transmitter frequency.

The Beam Steering Mirror:

The basic requirements of the beam steering mirror are a positioning accuracy of around 20 arcseconds and an ability to switch between positions separated by approximately 2 degrees in less than 70 ms. This follows from the requirement to measure five points per second on the surface of the GBT (we assume that adjacent measurement points will have a separation of one panel width). If we allow 128 ms integration time per point, then 72 ms remain for mirror movement and settling.

Motion in two orthogonal axes is provided by a simple two-axes mount, each axis being driven by a direct drive torque motor. Each axis position is sensed by an incremental encoder having a resolution of 10^5 pulses per revolution. A commercially-available servo controller card is used to complete a closed-loop servo for accurate positioning of the mirror and contains the hardware required to realize a high performance positioning servo without the need for velocity sensors or analog compensation.

The Phase Detection Method:

A 16-bit, analog-to-digital converter, synchronized to the 1 kHz reference signal, is used to sample the 1 kHz signal into a sequence of samples s_j . The Fourier components of the fundamental harmonic for retroreflector i are

$$a_i = \sum_{j=0}^{mn-1} s_j \cos\left(\frac{2\pi j}{n}\right)$$

$$b_i = \sum_{j=0}^{mn-1} s_j \sin\left(\frac{2\pi j}{n}\right)$$

where n = number of samples per cycle and m = number of cycles sampled.

The signal amplitude and phase are

$$A_i = \frac{2}{mn} (a_i^2 + b_i^2)^{1/2}$$

$$\phi_i = \tan^{-1} \left(\frac{b_i}{a_i} \right) .$$

In our case, the number of samples per cycle was chosen to be 64.

The effectiveness of this phase detection method is illustrated in Figure 7 which is a record of received amplitude and computed phase as the transmitted beam is scanned across a retroreflector. The computed distance remains constant over a change of amplitude in received signal of several orders of magnitude.

TESTS OF THE INSTRUMENT

After initial laboratory tests, the instrument was set up in an isolated building suitably equipped to transmit the laser beam over an outdoor horizontal path to a distant retroreflector mounted on an accurately calibrated translation stage. The first test performed was a measure of the linearity of the instrument as shown in Figure 8. This test was made at a range of 100 m with an integration time of one second per data point. The slope of the response was correct and the standard deviation of a single point was less than 20 microns, a very satisfactory value. There was no sign of the cyclical error that would be expected if there was RF leakage at the transmitter frequency into the receiver circuits.

The instrumental noise was investigated with results that are summarized in Figure 9, a plot of the standard deviation (RMS) on a range reading plotted against the number of intermediate frequency (IF) cycles per reading. The IF is 1 kHz; thus, 10 IF cycles is an integration time of 10 ms. The noise introduced by the data-taking circuitry is seen to be small, around 0.7 microns for 128 cycles. The noise in this case is seen to decrease as the square root of the integration time, as would be expected for random noise. A similar result is observed for the instrument measuring a short (1 meter) range, but in this case the noise is higher, around 6 microns for 128 ms.

The source of this higher noise was found to be due to phase noise on both the transmitter and local oscillator sources. This could undoubtedly be reduced, either by increasing the 1 kHz IF or by increasing the spectral purity of the oscillators, but the performance was judged to be more than adequate for this application. The final curve in Figure 9 shows a corresponding plot for a range of 30 m. In this case, atmospheric turbulence causes the phase fluctuations to decrease more slowly with integration time, $\tau^{-0.3}$ instead of $\tau^{-0.5}$, due to the Kolmogorov spectrum of phase variation with time for path lengths greater than the size of the turbulence cells [6].

Atmospheric turbulence consists of "bubbles" or "blobs" of air at slightly differing density to the surrounding air and is characterized by the so-called structure function, C_n^2 , which may be loosely considered a measure of the refractive index difference between the "blobs" and the surrounding air. Various references exist relating the structure function, C_n^2 , to variance in range measurement [4]. A large body of references also exists on the characteristics of C_n^2 ; a good summary is contained in [5].

The instrument was eventually set up to measure distance to a retroreflector at a range of 120 meters. Measurements were taken once per second with an integration time of 128 ms. Each minute the mean and RMS of the 60 measured ranges were calculated and stored. The values obtained for the RMS departures from the mean were then plotted as shown in Figure 10. In this example, the RMS values cluster around 20 microns, with no values over 50 microns. Over tests which continued for several months, RMS values varied from 9 microns to 45 microns. The lowest values occurred early on still, foggy mornings and generally the highest values on sunny afternoons.

The bulk refractive index of the atmosphere is greater than unity and over a path length of 100 meters, the corresponding reduction in group velocity leads to a measured path length that is around 30 mm longer than that which would be measured in a vacuum. The exact value of the group velocity depends on pressure, temperature and humidity [7]. Changes of several millimeters in the measured distance over a hundred-meter path are possible as a result of normal diurnal variations. However, due to the close proximity of the distances, all measurement paths should be affected equally, and the overall shape and pointing of the structure are therefore maintained. If absolute distances are required, then correction to the measured path lengths is possible by measuring the temperature, pressure, and relative humidity and computing a corresponding refractive index. This is common practice in commercial surveying instruments but may not be suitable for this application. A more practical solution would be to use the measured distances between the various fixed ground-based instruments and to scale all distances measured on the structure accordingly.

Of crucial importance is the homogeneity of the atmosphere. The change in refractive index must be the same over all measurement paths. In order to demonstrate this, at least in a preliminary way, the instrument was set up to measure two ranges separated by 15 degrees in azimuth, one range was 50 m, the other 120 m. The two ranges were measured and recorded once a minute for two days during which ambient conditions varied considerably. Figure 11 is a plot of each measurement point (with arbitrary zero point) and demonstrates that the changes in measured distance due to changes in group refractive index of the atmosphere are proportional to distance. The slope of the line is correct (12/5) and the standard deviation of a measurement point from this line is 18

microns. This error includes all sources of error; the stability of the monuments, for example, is included.

CONCLUSIONS

The prototype instrument described in this paper satisfies the basic requirements for measuring a large structure (approximately 100 m in diameter) with sufficient speed and accuracy to apply real-time corrections to an accuracy of better than 100 microns.

ACKNOWLEDGEMENTS

The authors would like to acknowledge R. Hall for support from the GBT Project, R. Creager and A. Dowd for software support, and R. Becker for help with the construction of the instrument. The contributions of the Green Bank machine shop are gratefully acknowledged, as are the many helpful suggestions from J. W. Findlay and D. Hogg.

REFERENCES

- [1] Simo H. Lavrila, *Electronic Surveying in Practice*, Wiley-Interscience, New York, 1983, pp. 248-250.
- [2] J. M. Payne, *Rev. Sci. Instrum.*, vol. 44, p. 304, 1973.
- [3] A. Greve and W. Hart, *Applied Optics*, vol. 23, p. 2982, 1984.
- [4] C. S. Gardner, *Applied Optics*, vol. 15, p. 2539, 1976.
- [5] D. L. Walters and K. E. Kienke, *J. Opt. Soc. Am.*, vol. 71, p. 397, 1981.
- [6] H. Matsumoto and K. Tsukahara, *Applied Optics*, vol. 23, p. 3388, 1984.
- [7] *Bergstrand Handbuch der Physik*, edited by S. Flugge, Springer-Verlag, Berlin, 1957, p. 1.

LIST OF FIGURES

Fig. 1. The geometry of the metrology system.

Fig. 2. The principle of the method.

Fig. 3. Block diagram of instrument.

Fig. 4. Schematic of laser diode transmitter RF section.

Fig. 5. Schematic of receiver section.

Fig. 6. Frequency generation.

Fig. 7. Range variation with received amplitude.

■ - received amplitude.

□ - measured distance.

Fig. 8. Instrument linearity.

Slope - 0.9997

Standard deviation on a single measurement - 20 microns.

Fig. 9. Noise contributions.

□ - phase detection circuits alone. Slope = -0.57.

▲ - range measurements, target retroreflector at 1 m. Slope = -0.57.

X - range measurements, target retroreflector at 31.5 m.

Slope = -0.34

Fig. 10. RMS noise at 100 m.

Fig. 11. Atmospheric effects. Slope = 0.41, RMS = 18.7 microns.

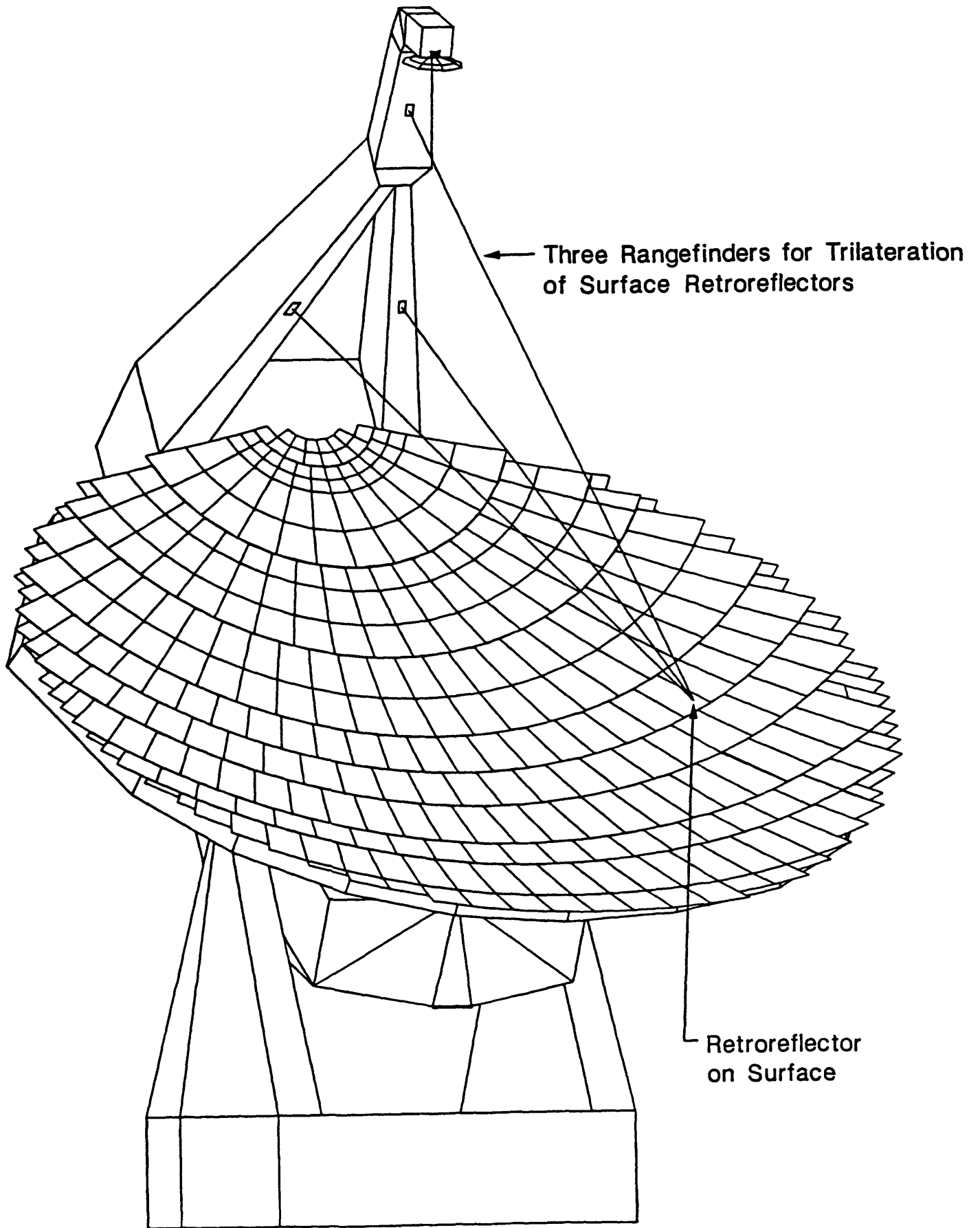


Fig. 1. The geometry of the metrology system.

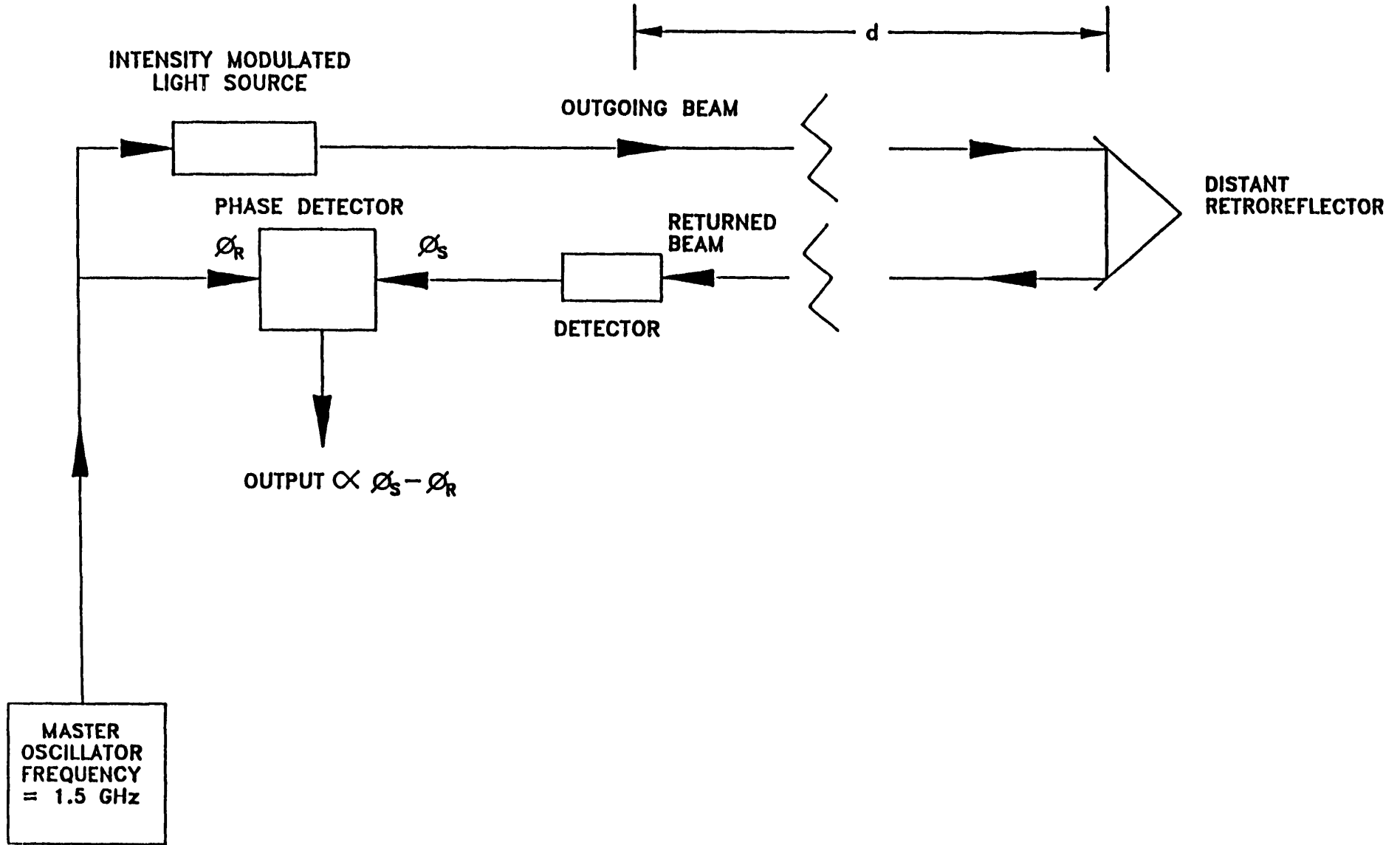


Fig. 2. The principle of the method.

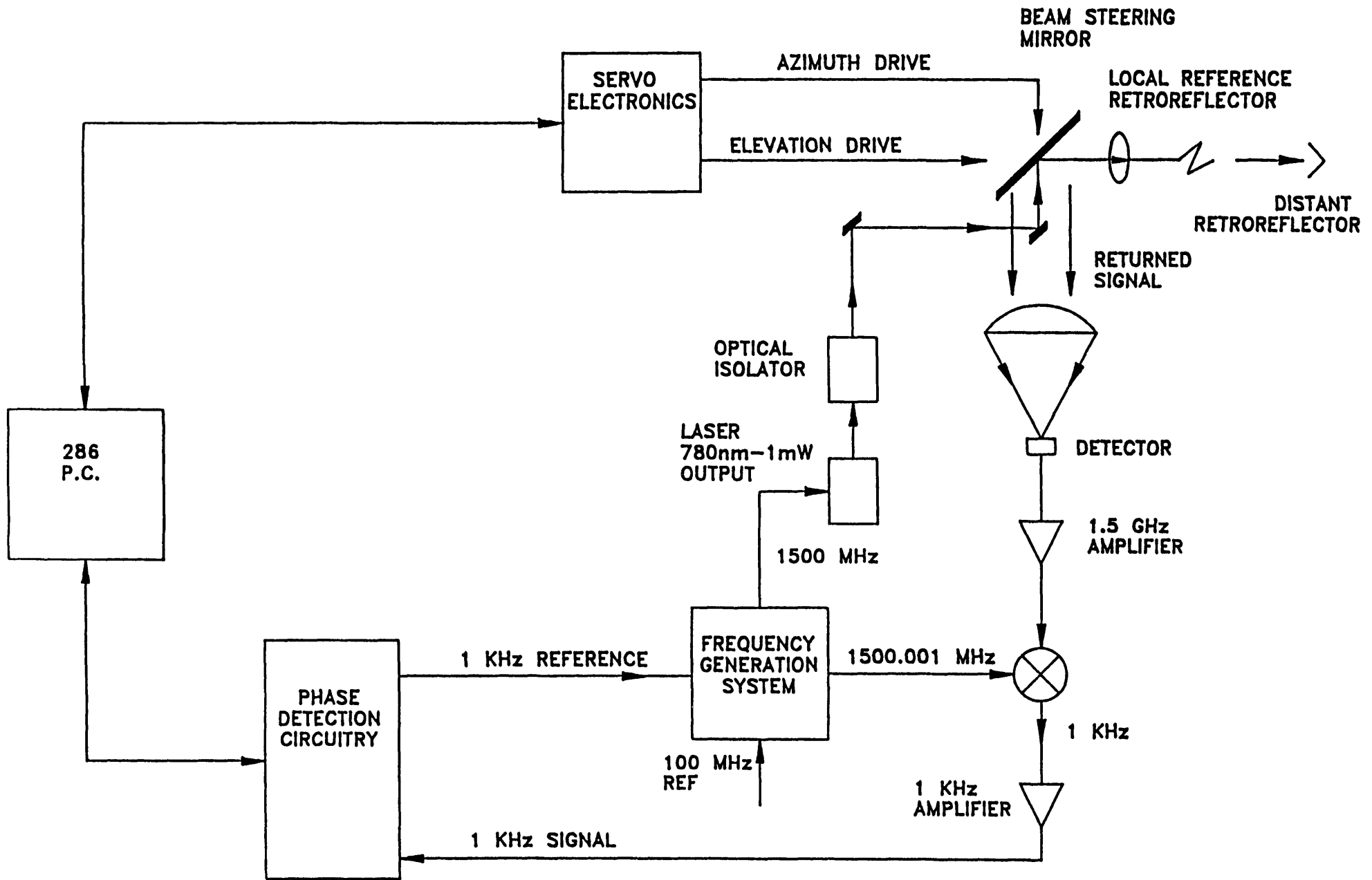


Fig. 3. Block diagram of instrument.

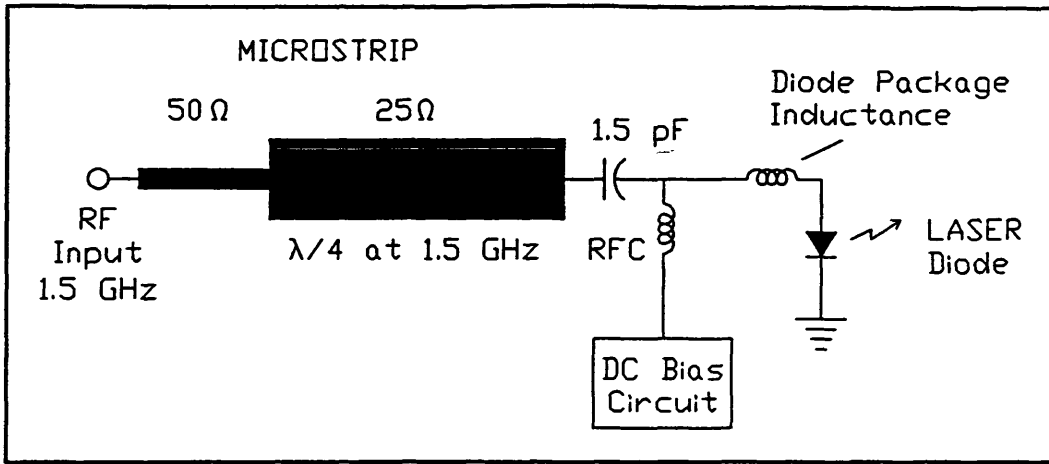


Fig. 4. Schematic of laser diode transmitter RF section.

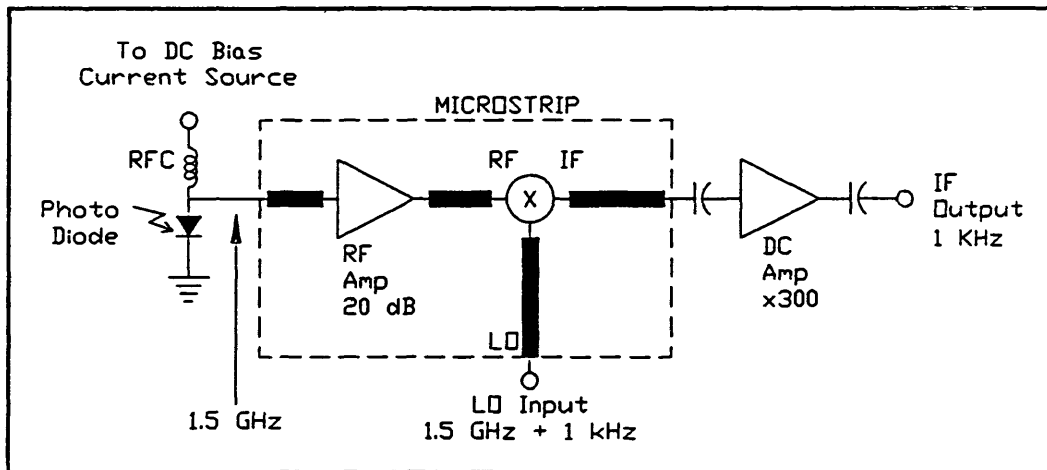


Fig. 5. Schematic of receiver section.

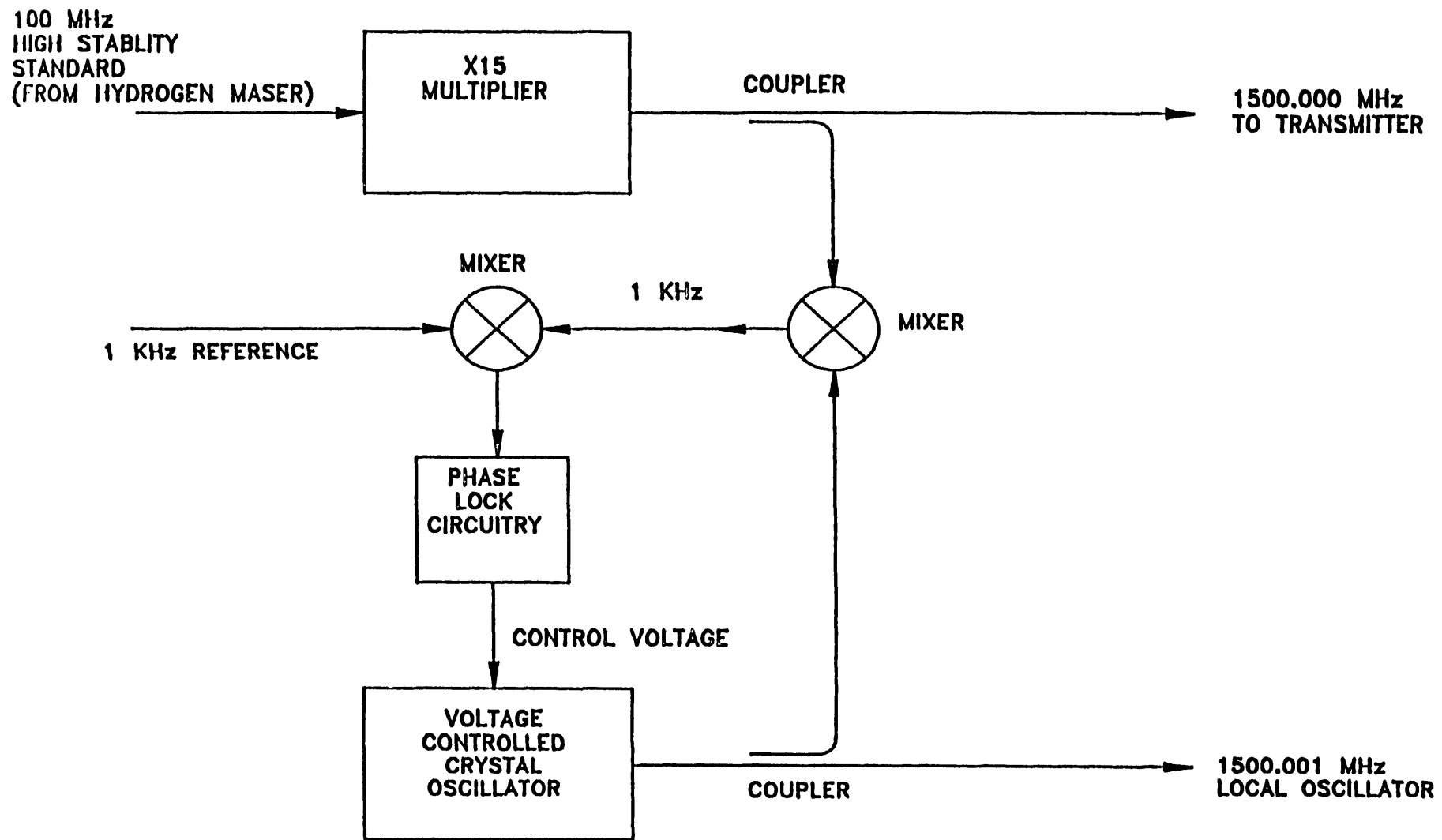


Fig. 6. Frequency generation.

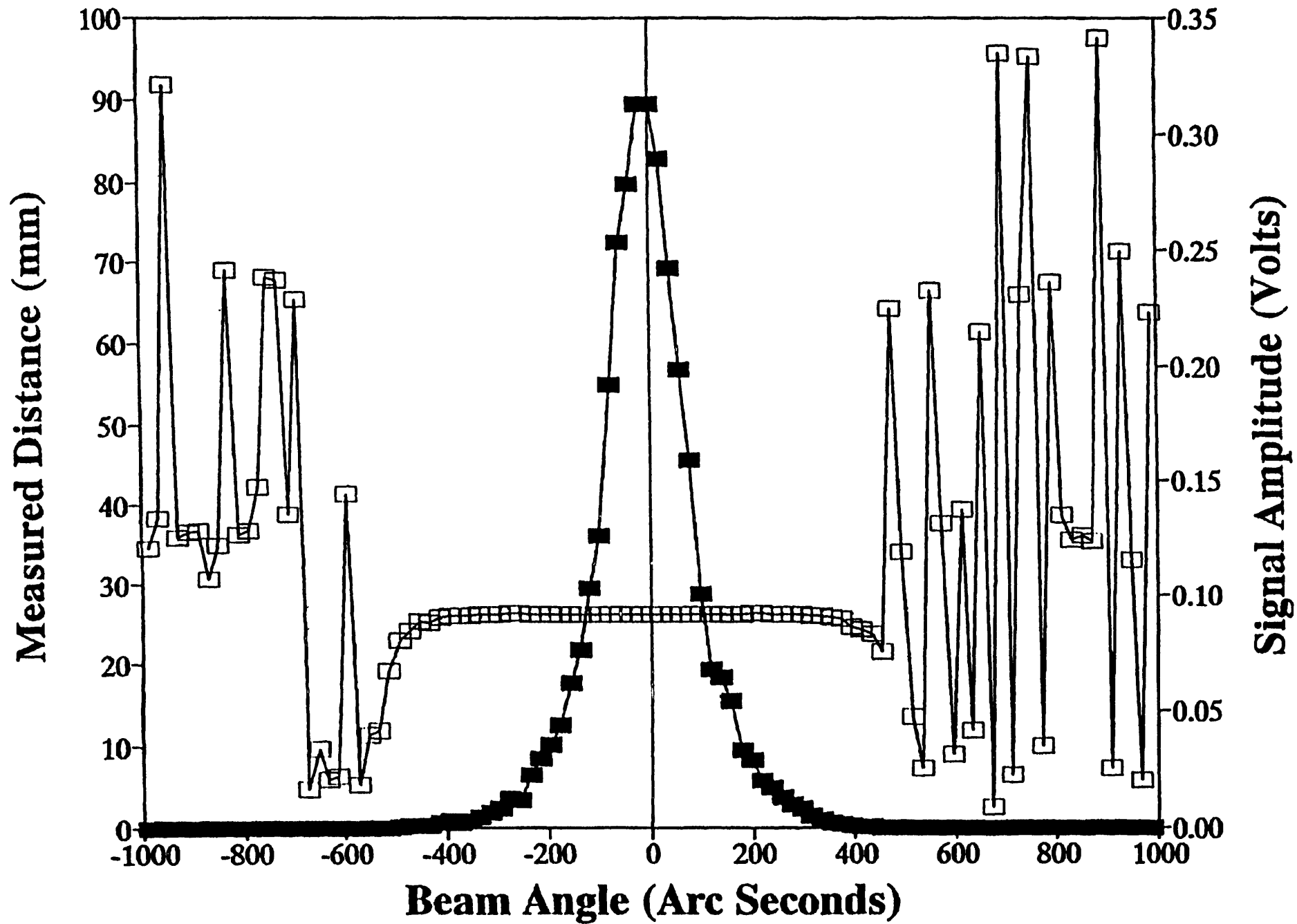


Fig. 7. Range variation with received amplitude.
 ■ - received amplitude.
 □ - measured distance.

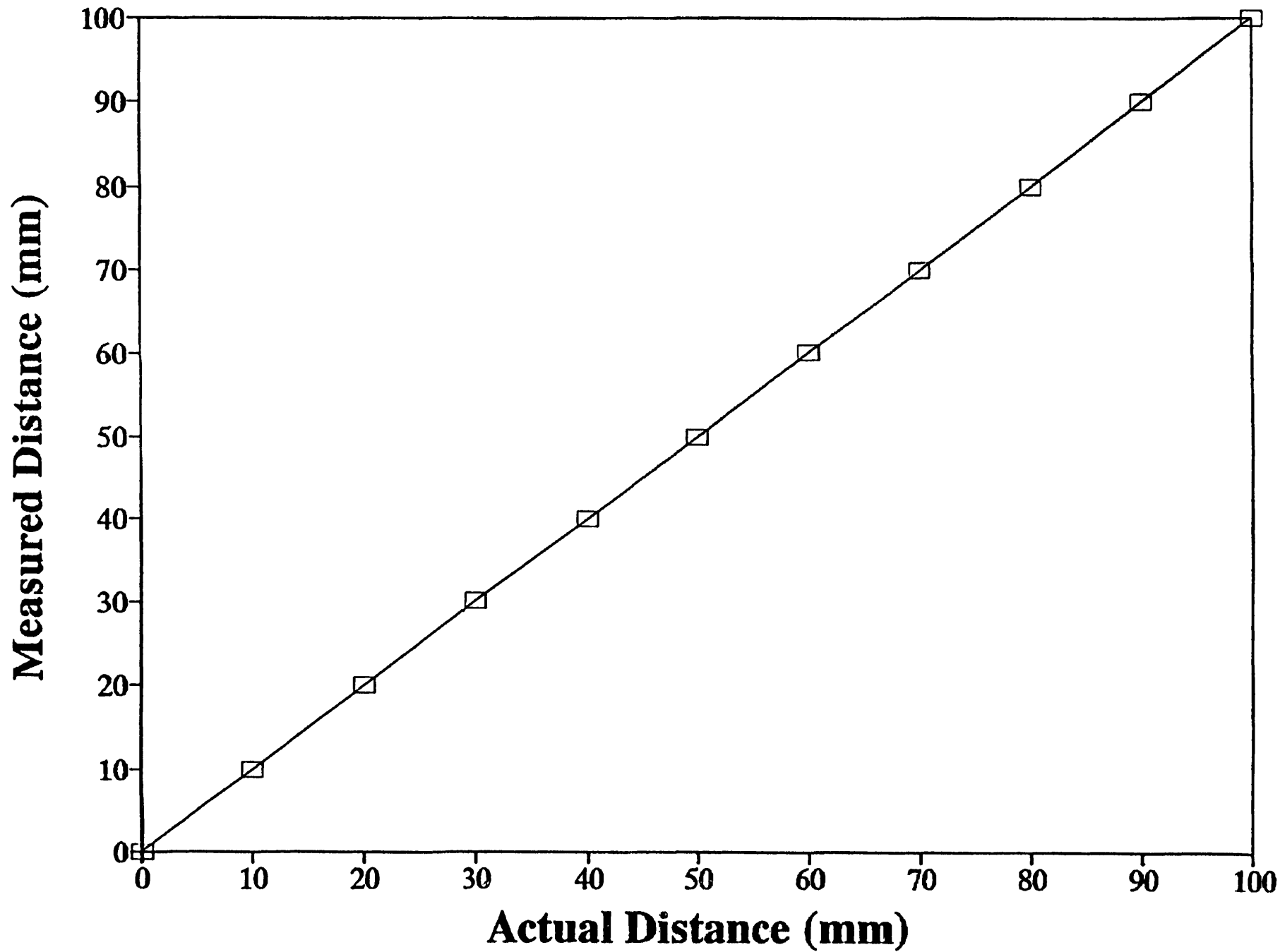


Fig. 8. Instrument linearity.
Slope - 0.9997
Standard deviation on a single measurement - 20 microns.

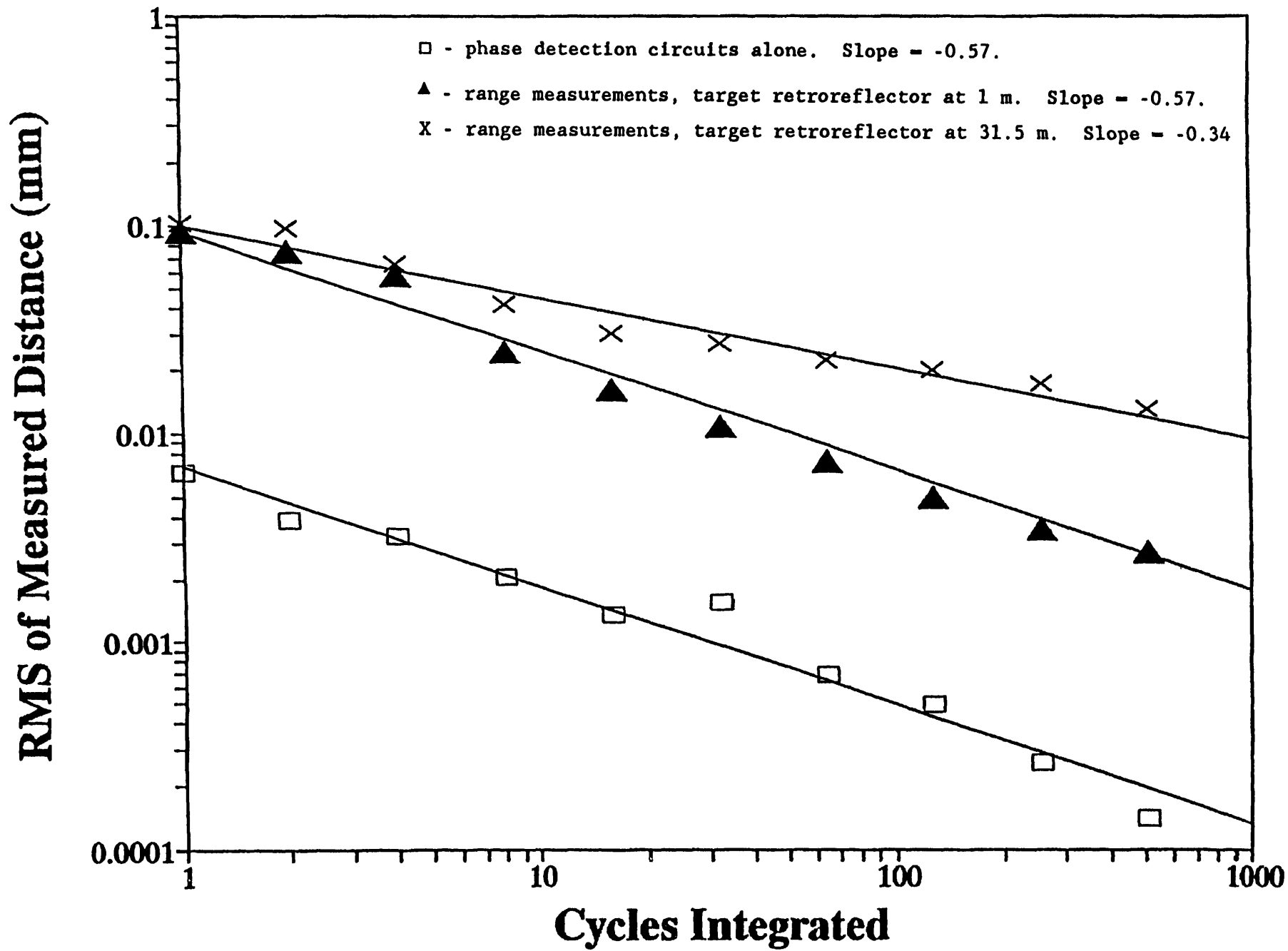


Fig. 9. Noise contributions.

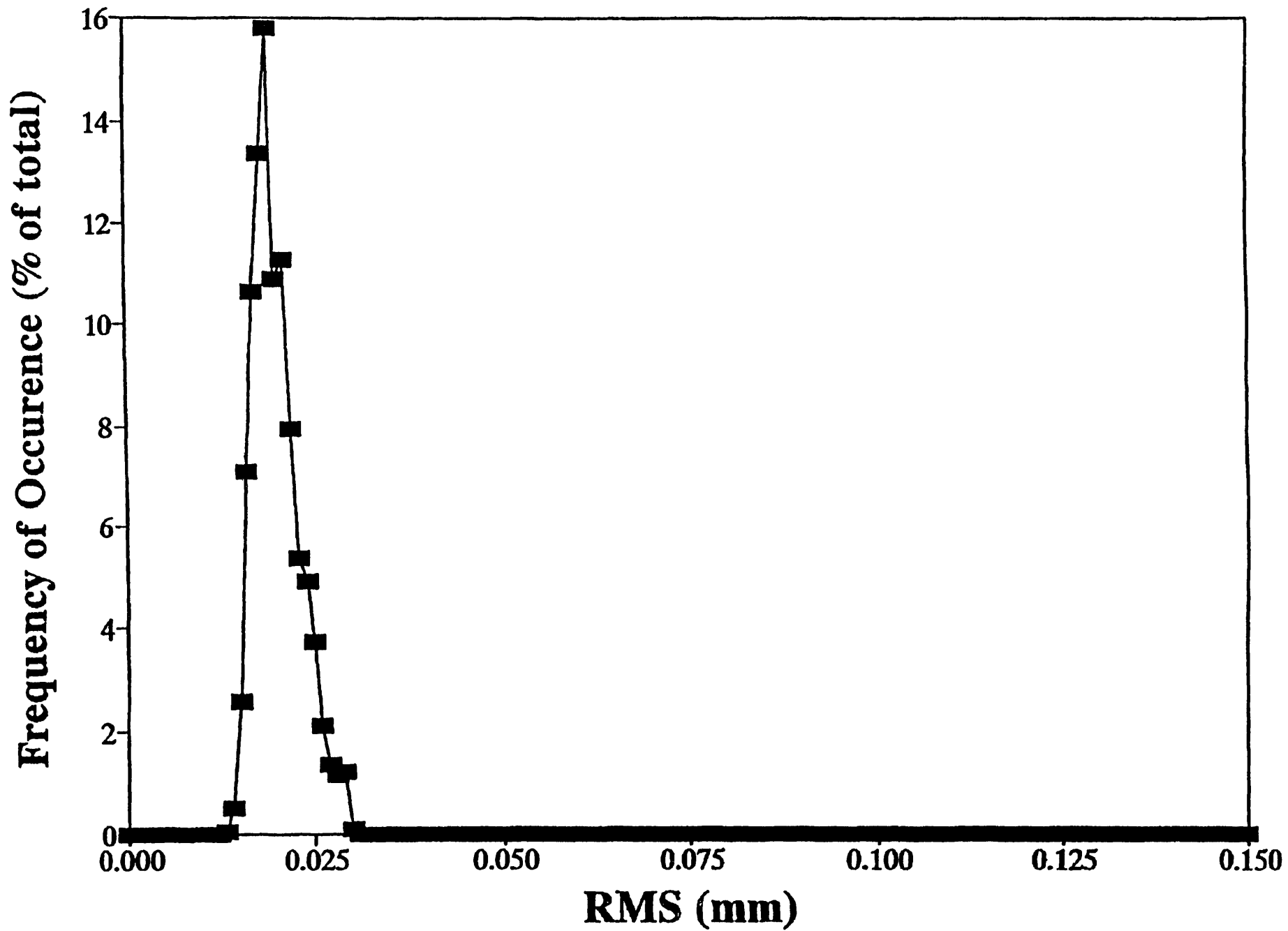


Fig. 10. RMS noise at 100 m.

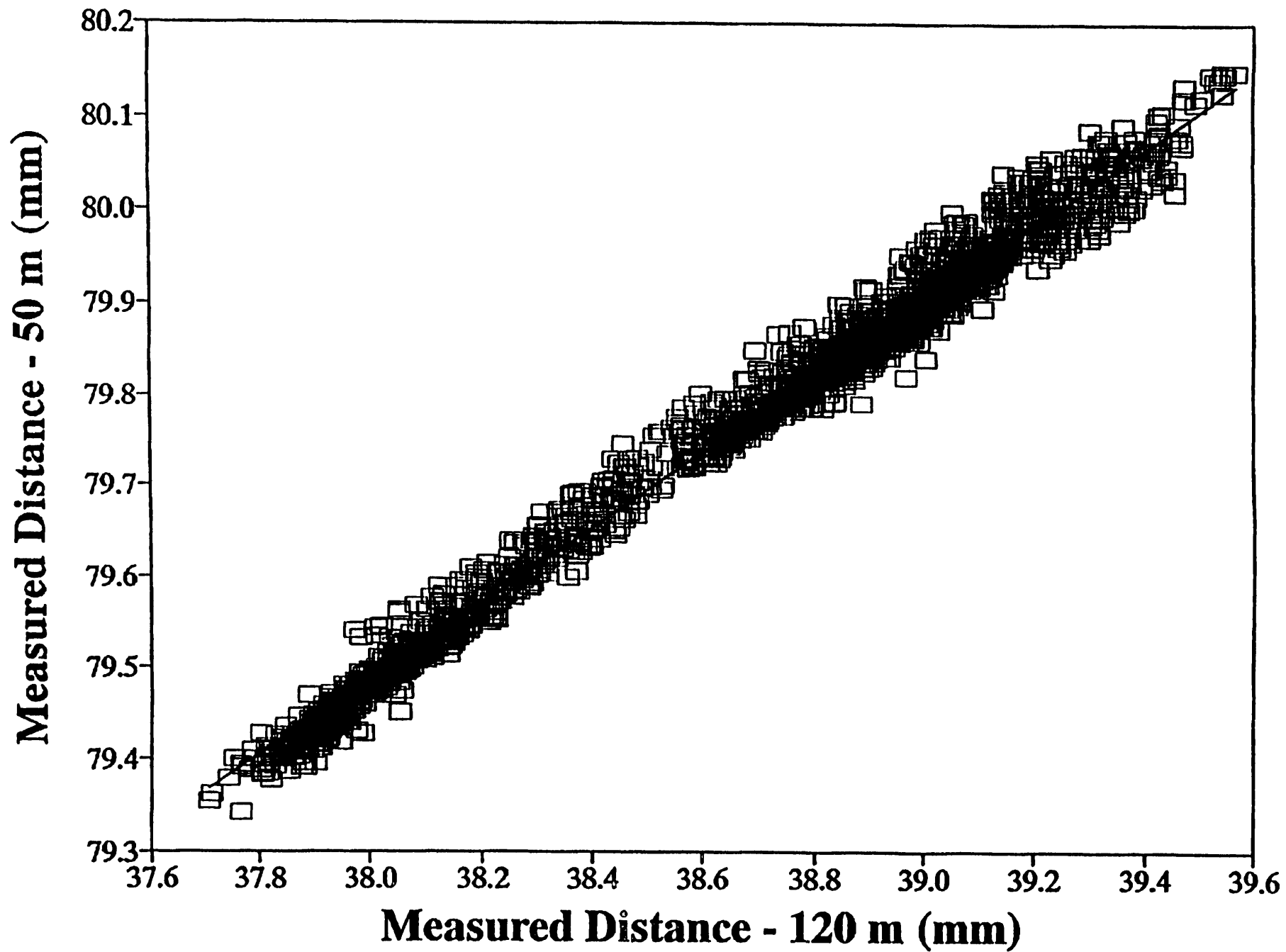


Fig. 11. Atmospheric effects. Slope = 0.41, RMS = 18.7 microns.